nitrogen

MDPI

Article

Comparative Effects of Iron Nanoparticles, Chelates, and Iron Sulfate on Biomass, Yield, and Nitrogen Assimilation in Spinach

Cristina L. Franco-Lagos [1], Eloy Navarro-León [2], Erick H. Ochoa-Chaparro [1], Celia Chávez-Mendoza [1], Ezequiel Muñoz-Márquez [1], Alexandro Guevara-Aguilar [1], Marina I. Terrazas-Gómez [3] and Esteban Sánchez [1,*]

[1] Food and Development Research Center, Avenida Cuarta Sur No. 3820 Fraccionamiento Vencedores del Desierto, Delicias 33089, Chihuahua, Mexico; cfranco123@estudiantes.ciad.mx (C.L.F.-L.); eriicktronik@hotmail.com (E.H.O.-C.); celia.chavez@ciad.mx (C.C.-M.); emunoz@ciad.mx (E.M.-M.); aguevara@ciad.mx (A.G.-A.)
[2] Department of Plant Physiology, Faculty of Sciences, University of Granada, 18071 Granada, Spain; enleon@ugr.es
[3] Faculty of Agricultural and Forestry Sciences, Autonomous University of Chihuahua, Campus Delicias, Km 2.5 Road to Rosales, Chihuahua 33000, Chihuahua, Mexico; miterrazas@uach.mx
* Correspondence: esteban@ciad.mx; Tel.: +52-639-549-4681

Abstract

Foliar application with iron is a promising strategy for improving nitrogen nutrition and productivity in horticultural crops. In this study, the effect of the foliar application of iron oxide nanoparticles (IONPs) compared to conventional iron sources on physiological, biochemical, and productive parameters of *Spinacia oleracea* L. was evaluated. Plants were treated with different concentrations (0, 25, 50, and 100 ppm) of IONPs, ferric sulfate (FS), and iron chelate (IC). Biomass, yield, nitrate reductase enzyme activity, soluble protein and amino acid contents, SPAD values, and photosynthetic pigments were analyzed. The results showed that IONPs, particularly at 50–100 ppm, promoted significant increases in biomass (50% more than the control), yield (47%), and nitrate reductase enzyme activity (NR_{max}) (246%) compared to the control (0 ppm) without negatively affecting pigment levels or leaf physiological condition. Likewise, increases in soluble protein and photosynthetic pigment levels were observed, reflecting improved nitrogen assimilation and photosynthetic efficiency. These findings suggest that IONPs represent an efficient and safe alternative to traditional Fe sources, contributing to the development of sustainable agricultural systems aimed at improving the nutritional value and productivity of leafy crops.

Keywords: nanoparticles; foliar micronutrient application; *Spinacia oleracea* L.; sustainable agriculture

Academic Editor: Germán Tortosa

Received: 23 June 2025
Revised: 8 August 2025
Accepted: 4 September 2025
Published: 8 September 2025

Citation: Franco-Lagos, C.L.; Navarro-León, E.; Ochoa-Chaparro, E.H.; Chávez-Mendoza, C.; Muñoz-Márquez, E.; Guevara-Aguilar, A.; Terrazas-Gómez, M.I.; Sánchez, E. Comparative Effects of Iron Nanoparticles, Chelates, and Iron Sulfate on Biomass, Yield, and Nitrogen Assimilation in Spinach. *Nitrogen* **2025**, *6*, 81. https://doi.org/10.3390/nitrogen6030081

1. Introduction

The growing pressure on agricultural systems resulting from climate change, population growth, and the need for intensified food production highlights the urgent necessity to implement more sustainable and efficient nutrient management strategies. Among essential nutrients, iron (Fe) and nitrogen (N) play critical roles in sustaining crop productivity, particularly in horticultural systems [1,2].

The N assimilation process involves the absorption of nitrate (NO_3^-) and ammonium (NH_4^+), followed by their reduction and conversion into amino acids through the enzymatic pathways of nitrate reductase (NR), nitrite reductase (NiR), glutamine synthetase (GS), and glutamate synthetase (GOGAT) [3]. Fe is a key micronutrient in these pathways, acting as

an essential cofactor in nitrate reduction enzymes and in proteins such as ferredoxin, which are essential for electron transport during photosynthesis and NO_3^- reduction [4,5].

Despite the abundance of Fe in soils, its availability to plants is limited due to its low solubility, especially in calcareous or high pH soils [5]. Therefore, the efficient management of Fe and N is a technical and environmental challenge. In this context, the use of metal-oxide nanoparticles, such as iron oxide nanoparticles (IONPs), and the development of nano-biofertilizers represent significant advances in improving mineral nutrition and crop resilience to adverse conditions. These innovative technologies increase the availability of iron in the rhizosphere and its translocation within the plant, promoting essential physiological processes such as photosynthesis, chlorophyll synthesis, and nitrate reduction [6,7]. The application of IONPs and nano-fertilizers based on iron-loaded algal biomass has been shown to increase yield, amino acid content, and iron levels in crops of agricultural interest [8]. Likewise, recent studies have highlighted that these nanoparticles can improve growth, nutrient absorption, and antioxidant balance in horticultural species, even under saline stress or in low-fertility soils [6,9]. In addition, research in horticultural systems has shown that nanostructured biofertilizers can optimize nitrogen and other nutrient metabolism, contributing to a better physiological and productive performance [10].

Different Fe sources have distinct physicochemical properties that influence their mobility, solubility, and efficiency in plant systems [4]. For example, iron chelate (Fe-EDDHA) is a synthetic compound designed to remain soluble even under high pH conditions [2], ferric sulfate ($Fe_2(SO_4)_3$) is a common inorganic salt but has limited availability under alkaline conditions [11], and iron oxide nanoparticles (IONPs) represent an emerging technology with enhanced surface area and reactivity, potentially improving foliar absorption and translocation [12]. These contrasting properties may significantly influence plant physiological responses, particularly under nutrient-limited conditions.

Several studies have reported that metal nanoparticles and their derivatives can improve biomass, photosynthetic pigments, and nitrogen compounds in crops such as lettuce and tomato [13]. Recent research has also demonstrated that zinc oxide nanoparticles (ZnO NPs) significantly enhance biomass production, chlorophyll content, and antioxidant responses in rice under stress conditions, supporting their multifunctional role in crop physiology [14]. However, in leaf crops with high nutritional demands such as spinach (Spinacia oleracea), research on the effect of IONPs on N assimilation and physiological indicators such as free amino acids and soluble proteins is still scarce [15]. This information is key to understanding the role of nanoparticles in primary N metabolism and their potential to optimize nutrition in sustainable agricultural systems.

Therefore, the objective of this study was to evaluate the effect of foliar application of IONPs compared to conventional sources of Fe, iron chelate (Fe-EDDHA), and ferric sulfate ($Fe_2(SO_4)_3$) on biomass, yield and N assimilation in spinach (*Spinacia oleracea* L. cv. Viroflay). We hypothesized that foliar application of IONPs would enhance nitrogen assimilation efficiency, resulting in higher concentrations of free amino acids, soluble proteins, and biomass compared to conventional Fe sources.

2. Materials and Methods

2.1. Experimental Site and Crop Management

The experiment was conducted at the Food and Development Research Center (CIAD) in Delicias, Chihuahua, Mexico, from April to May 2023, under greenhouse conditions with shade netting and an average temperature of 32.48 °C. Seeds of *Spinacia oleracea* L. cv. Viroflay were used.

Germination was carried out in polystyrene trays with vermiculite as substrate, applying 250 mL of nutrient solution prepared with distilled water every three days for 30 days.

Twenty-four days after sowing (DAS), the seedlings were transplanted into 5 L plastic pots using a 2:1 (v/v) mixture of vermiculite and perlite as substrate.

The irrigation system used was passive hydroponics, using subirrigation in plastic trays (33 × 55 × 4 cm), where the pots were placed directly on a constant layer of nutrient solution. This system allowed water and nutrients to rise by capillary action from the base of each pot, ensuring a uniform and efficient supply without wetting the foliage [16]. During the trial, a nutrient solution composed of 6 mM NH_4NO_3, 1.6 mM K_2HPO_4, 0.3 mM K_2SO_4, 4.0 mM $CaCl_2 \cdot 2H_2O$, 1.4 mM $MgSO_4 \cdot 7H_2O$, 2 µM $MnSO_4 \cdot H_2O$, 1.0 µM $ZnSO_4 \cdot 7H_2O$, 0.25 µM $CuSO_4 \cdot 5H_2O$, 0.3 µM $(NH_4)_6Mo_7O_{24} \cdot 4H_2O$, and 0.5 µM H_3BO_3 was adjusted to a pH of 6.0 ± 0.1 [17]. One liter of solution was applied per pot every 24 h from transplanting, 24 DAS, until harvest, 60 DAS.

2.2. Characterization of Iron Oxide Nanoparticles IONPs

For this study, iron oxide nanoparticles (Fe_2O_3 NPs) were obtained from the Mexican company Investigación y Desarrollo de Nanomateriales S.A. de C.V., synthesized via a wet chemical method. According to the technical data sheet, the nanoparticles are composed of the maghemite phase (γ-Fe_2O_3), a magnetic and semiconducting polymorph of Fe_2O_3. The particles have a reddish fine powder appearance, an average particle size below 50 nm, and a chemical purity of 99.7%.

Structural and morphological characterization was carried out by X-ray diffraction (XRD), confirming the crystalline structure of maghemite. Scanning electron microscopy (SEM) and transmission electron microscopy (TEM) revealed spherical to quasi-spherical shapes, with moderate polydispersity and a size consistent with the nominal specification (Figures 1 and 2). Additionally, energy-dispersive X-ray spectroscopy (EDX) (Figure 3) analysis confirmed the elemental composition corresponding to iron and oxygen without traces of other contaminants.

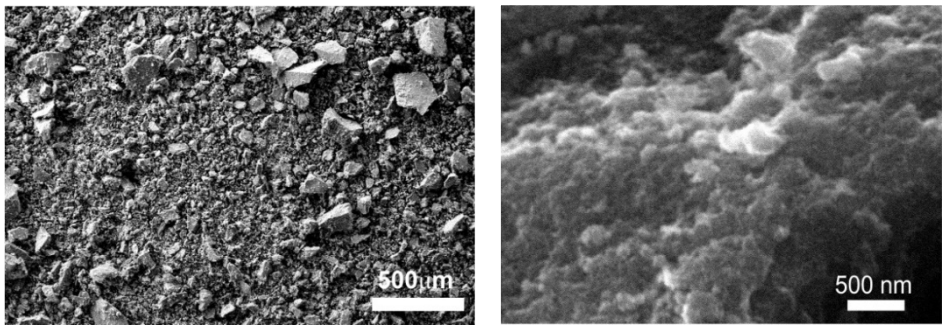

Figure 1. Sample morphology by scanning electron microscopy (SEM).

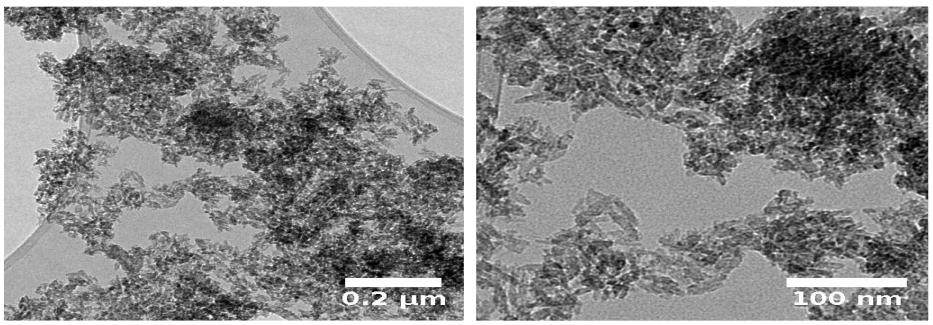

Figure 2. Sample morphology by transmission electron microscopy (TEM).

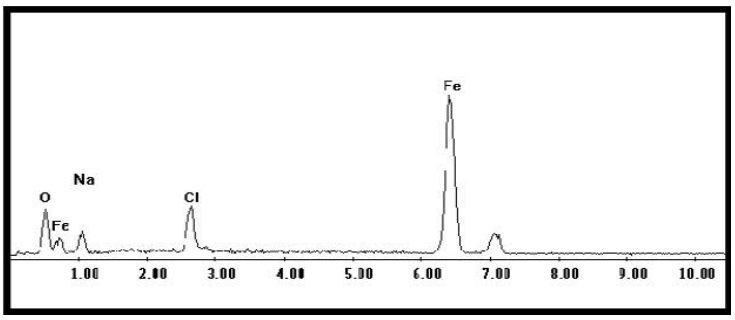

Figure 3. Elemental analysis (chemical composition) by X-ray energy dispersive spectroscopy (EDX).

Although parameters such as specific surface area (BET) and zeta potential were not determined, the physicochemical properties provided by the manufacturer indicate high-quality nanomaterials suitable for foliar application, ensuring consistent dispersion and bioavailability in plant systems.

2.3. Nanoparticles Preparation

A stock solution of IONPs was prepared at a concentration of 100 ppm using triple-distilled water as the solvent. The mixture was homogenized by mechanical stirring on a magnetic plate (VWR® International Model 150D) at 700 rpm for 20 min and then sonicated in an ultrasonic bath (Vevor Ultrasonic Cleaner, Cleveland, OH, USA) at a frequency of 40 kHz for 15 min at a controlled temperature of 25–30 °C, following the protocol described by Waqas et al. [18]. The working concentrations (25, 50, and 100 ppm) were obtained by appropriate dilutions of the stock solution.

2.4. Experimental Design and Treatments

A completely randomized experimental design with a single-factor arrangement was used, consisting of three iron sources: ferric sulfate $Fe_2(SO_4)_3$, iron chelate (Fe-EDDHA), and IONPs, applied at concentrations of 0, 25, 50, and 100 ppm (Table 1). Each treatment had four replicates, and the experimental unit consisted of a single plant grown in a 5 L plastic pot. Once transplanted to pots 25 DAS, the treatments were applied foliar to the point of dripping, with a total of four applications made at weekly intervals under controlled conditions throughout the crop cycle.

Table 1. Description of treatments (iron source and concentration).

Concentration (ppm)	Ferric Sulfate $Fe_2(SO_4)_3$	Iron Chelate (Fe-EDDHA)	IONPs (Fe_2O_3)
0	Control	Control	Control
25	FS25	IC25	IONPs25
50	FS50	IC50	IONPs50
100	FS100	IC100	IONPs100

2.5. Plant Sampling

Once the plants reached physiological maturity at 60 DAS, the plant material was harvested. The collected material was washed with distilled water to remove residues and finally separated into organs (root and leaves). The samples were divided into fresh and dry material. The fresh material was used to determine yield, nitrate reductase enzyme activity, and the concentration of photosynthetic pigments, amino acids, and soluble proteins. The dry material was used to quantify biomass.

2.6. Plant Analysis

2.6.1. Biomass and Yield

To quantify total biomass and yield, four plants per treatment were randomly selected and weighed fresh using a compact balance (A&D Co., Ltd., EK-120, Tokyo, Japan). The plants were then dissected into leaves and roots, and the fresh weight of each organ was recorded separately.

Yield was calculated as the average fresh weight of leaves per plant (g plant^{-1} FW). The organs were rinsed three times with distilled water and left to dry at room temperature on absorbent paper for 24 h.

After this period, two plants from each treatment were dried in a laboratory oven with forced air circulation (Shel-Lab 1380FX, Cornelius, OR, USA) with a volume of 13.9 cubic feet at 45 °C for 72 h [19].

Finally, the samples were weighed on an electronic analytical balance (A&D Co., Ltd., HR-120, Tokyo, Japan). Total biomass was expressed as the sum of the dry weight of the leaves and roots (g plant^{-1} DW).

2.6.2. Analysis of Photosynthetic Pigments

The method used for pigment extraction and quantification from the leaf was described by Wellburn [20]. The total chlorophyll concentration was quantified by extraction with methanol and absorbance measurements. Leaf disks with a diameter of 7 mm, corresponding to 0.15 g of fresh plant material (leaves), were weighed and placed in test tubes with 10 mL of pure methanol (CH_3OH). The samples were sealed and left to stand in the dark for 24 h. After this time, the absorbance of the samples was measured at wavelengths of 470, 653, and 666 nm for carotenoids, chlorophyll b, and chlorophyll a, respectively, using a UV-visible spectrophotometer (Thermo Fisher Scientific, GENESYS™ 10S, Madison, WI, USA). Pigment concentrations were expressed in μg cm^{-2} FW and calculated using the following formulas:

$$\text{Chl a*} = [15.65 \times (\text{A666})] \times [7.34 \times (\text{A653})]$$

$$\text{Chl a} = (\text{Chl a*} \times \text{Vf} \times \text{W1})/(\text{W2} \times \pi \times \text{r}^2 \times \text{n}) \quad (1)$$

$$\text{Chl b*} = [27.05 \times (\text{A653})] - [11.21 \times (\text{A666})]$$

$$\text{Chl b} = (\text{Chl b*} \times \text{Vf} \times \text{W1})/(\text{W2} \times \pi \times \text{r}^2 \times \text{n}) \quad (2)$$

$$\text{Carotenoids*} = [(1000 \times (\text{A470})] - (2.86 \times \text{Chl a}) - (129.2 \times \text{Chl b}))/221$$

$$\text{Carotenoids} = (\text{Carotenoids*} \times \text{Vf} \times \text{W1})/(\text{W2} \times \pi \times \text{r}^2 \times \text{n}) \quad (3)$$

$$\text{Total chlorophyll} = \text{Chl a} + \text{Chl b} \quad (4)$$

A: absorbance; Vf: final volume; W1: weight per leaf disk; W2: total weight of leaf disks; r: radius of leaf disks; and n: number of leaf disks.

2.6.3. Chlorophyll Index

The relative chlorophyll content was determined using the SPAD (Soil–Plant Analysis Development) index, using a portable SPAD-502 chlorophyll meter (Konica Minolta Sensing, Inc., Osaka, Japan). This instrument allows non-destructive measurements of leaf greenness, which is considered an indirect indicator of chlorophyll content [21]. The results were expressed in SPAD units. The measurement was carried out at 50 DAS.

2.6.4. Extraction and Assay of NR

Frozen leaf tissue was homogenized by grinding leaves (midrib removed) or leaf disks (blotted with soft paper tissues) in a precooled mortar in liquid nitrogen. Extraction buffer (2 mL g^{-1} fresh w.) was added to the leaf powder and grinding continued until thawed. The extraction buffer contained 50 mM HEPES-KOH pH 7.6, 1 mM DTT, 10 µM FAD, and 1 mM EDTA. The homogenate was cleared by centrifugation (16,000× *g*, 5 min), and where mentioned, it was desalted by centrifugal filtration on Sephadex G25 spin columns equilibrated with buffer. The different activation states of NR were determined by assaying NR for 3 min either with Mg^{2+} (l0 mM) or with EDTA (15 mM) or after preincubation (30 min) with EDTA (15 mM) plus AMP (5 mM) plus KH_2PO_4 (10 mM) and assayed in EDTA buffer. In all cases, an aliquot (100 µL) of the extract was added to 900 µL of the reaction medium, which contained 50 mM HEPES-KOH pH 7.6, 1 mM DTT, 10 µM FAD, 5 mM KNO_3, and 10 mM $MgCl_2$ or 15 mM EDTA. Reaction was stopped after 3 min by addition of zinc acetate solution, as previously described by Kaiser and Brendle-Behnisch [22]. As leaves or leaf tissues accumulated considerable amounts of nitrite during some treatments, aliquots of the extracts were routinely assayed for nitrites, which was subtracted from the nitrite produced during the in vitro NR reaction.

2.6.5. Determination of Soluble Amino Acids

The concentration of soluble amino acids was determined using the Yemm and Cocking method [23] with adaptations. Approximately 0.5 g of fresh material was homogenized in 5 mL of 50 mM phosphate buffer (pH 7.0). The extract was filtered, centrifuged at 12,360× *g* for 15 min, and the supernatant was used for analysis. To 100 µL of supernatant, 1.5 mL of ninhydrin reagent was added and incubated in a water bath at 100 °C for 20 min. After cooling on ice, 8 mL of 50% propanol was added and allowed to stand for 30 min before reading at 570 nm. The concentration was calculated against a standard glycine curve and expressed in mg g^{-1} of fresh weight.

2.6.6. Determination of Soluble Proteins

Soluble protein was quantified from the same extract used for amino acids, using the Bradford method [24]. Twenty microliters of the extract were added to 1 mL of Bradford reagent, and the absorbance was measured at 595 nm, using a standard curve of bovine serum albumin (BSA). The results were expressed as mg g^{-1} of fresh weight.

2.7. Statistical Analysis

Once the data had been obtained, it was subjected to a Shapiro–Wilk test to check the normality of the distribution. In addition, it was subjected to a Bartlett test to check the homogeneity of the variances. Once the assumptions had been checked, the data was subjected to a one-way analysis of variance, followed by a test of separation of means using Fisher's LSD test. The statistical package SAS 9.0 was used for statistical analyses [25].

3. Results and Discussion

3.1. Biomass

One of the key parameters for evaluating nutrient efficiency is biomass accumulation, as it reflects the plant's ability to convert available nutrients into organic matter [26]. This indicator is crucial for crops because it integrates the effect of nutrients on plant growth and total yield [27]. In the present study, the foliar application of iron (Fe) in different forms and concentrations had different effects on dry biomass (g $plant^{-1}$) (Figure 4).

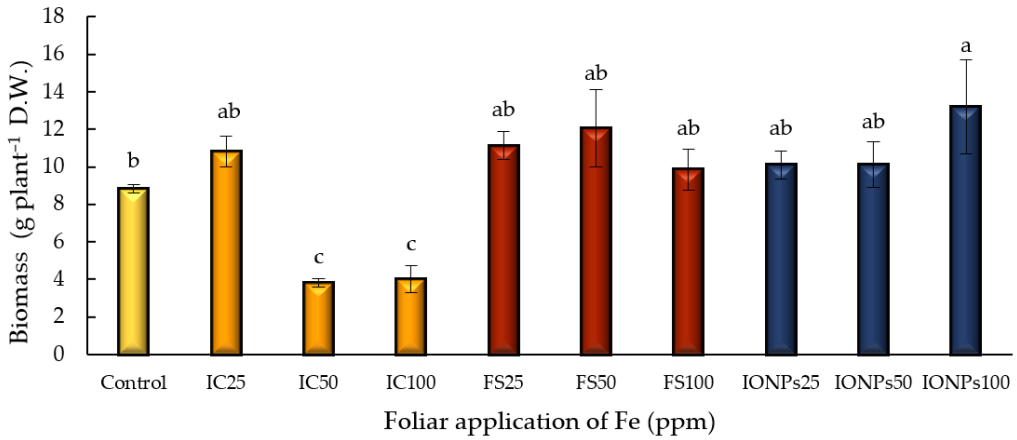

Figure 4. Effect of foliar application of iron chelate (Fe-EDDHA), ferric sulfate ($Fe_2(SO_4)_3$), and iron oxide nanoparticles (IONPs) on the biomass of *Spinacia oleracea* L. cv. Viroflay. Different letters represent significant differences between treatments according to Fisher's LSD test ($p \leq 0.05$).

The control had a value (100%) of approximately 8.81 g plant^{-1}. The highest biomass was obtained with IONPs100, with an increase of 49.8%, reaching about 13.2 g plant^{-1}. This was followed by FS50, with an increase of 36.7% and FS25 and IC25, with increases of 26.25% and 22.7%, respectively. In contrast, the IC50 and IC100 treatments reduced biomass by 56.7% and 54.3%, respectively, while IONPs25, IONPs50, and FS100 showed moderate improvements of approximately 14% compared to the control.

Interestingly, although Fe-EDDHA (IC) is commonly considered an effective source of iron due to its high solubility and stability under alkaline conditions [2], our results showed a decrease in biomass and yield with increasing IC concentrations. The highest dose (IC100) resulted in the lowest values among all treatments, possibly due to physiological imbalances caused by excess foliar iron [28]. Notably, the lowest dose of IC (25 ppm) produced biomass and yield levels comparable to those of IONPs100, suggesting that, at low concentrations, IC can still be effective. These findings highlight the importance of optimizing the dosage in foliar iron fertilization strategies.

The increases observed with IONPs can be attributed to their greater bioavailability and foliar penetration capacity, which optimizes photosynthetic activity, nitrogen metabolism, and redox balance, key factors in biomass accumulation [28,29]. Fe nanoparticles have also been shown to improve mineral distribution and antioxidant activity, reducing oxidative damage [12]. In contrast, treatments with high concentrations of conventional Fe salts may have caused osmotic stress or ionic toxicity, limiting growth [30]. These results are consistent with recent studies highlighting the potential of Fe nanoparticles to improve physiological and photosynthetic parameters in various crops [31].

3.2. Yield

Iron is a micronutrient necessary for various physiological and biochemical processes, such as photosynthesis, respiration, and nitrogen metabolism. Therefore, its application represents a key strategy for optimizing crop yield [32]. In the present study, the foliar application of iron (Fe) in different forms and concentrations significantly impacted the fresh yield (g plant^{-1} f.w.) (Figure 5). The control had a yield of approximately 75 g plant^{-1} (100%). The highest response was observed with IONPs100, with a 40% increase over the control (around 105 g plant^{-1}). This was followed by IC25 and FS25, which increased the yield by 28% and 13%, respectively. The treatments with IONPs25 and IONPs50 showed increases of 10% and 8%. In contrast, IC50 and IC100 reduced the yield by 7% and 34%, respectively, while FS50 showed a reduction of 11%.

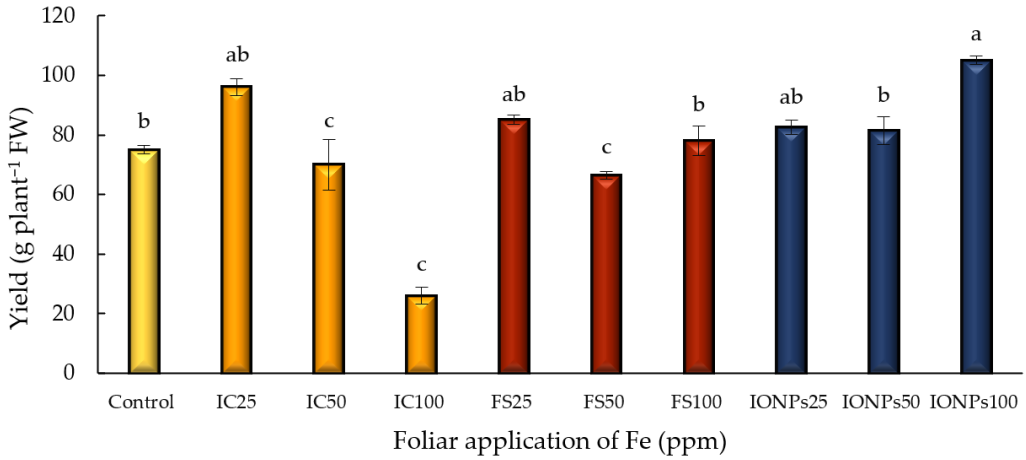

Figure 5. Effect of foliar application of iron chelate (Fe-EDDHA), ferric sulfate ($Fe_2(SO_4)_3$), and iron oxide nanoparticles (Fe_2O_3) on the yield of *Spinacia oleracea* L. cv. Viroflay plants. Different letters represent significant differences between treatments according to Fisher's LSD test ($p \leq 0.05$).

These results highlight the potential of Fe nanoparticles to improve crop yields due to their high bioavailability and efficient translocation to metabolically active tissues, favoring physiological processes such as photosynthesis and nitrogen assimilation [28]. According to [33], the foliar application of iron oxide (Fe_2O_3) NPs showed a 47% increase in chickpea crop yield compared to the control. Similarly, Dola et al. [34] reported that foliar application of iron oxide (Fe_3O_4) nanoparticles on soybeans increased the seed yield by 32–40% compared to the control. These results emphasize that the application of NPs not only increases nutrient availability but also facilitates the activation of physiological processes such as chlorophyll synthesis, photosynthetic activity, and factors that are reflected in higher yields [35]. In addition, the rapid release and availability of Fe in its nanoparticle form can induce elevated metabolic responses in crops, promoting proper growth, vegetative development, and higher productivity [36] compared to the conventional sources applied in this experiment.

The decreases observed in treatments with high concentrations of conventional Fe may be associated with osmotic stress or phytotoxicity, phenomena previously reported in other crops [30]. These observations are consistent with the findings of [31], who demonstrated that Fe nanoparticles optimize both productivity and photosynthetic rates in plants.

3.3. Photosynthetic Pigments

Iron plays an essential role in the synthesis of photosynthetic pigments, as it is necessary for chlorophyll biosynthesis and the proper functioning of chloroplasts, which directly impacts the photosynthetic efficiency of plants [37]. In the present study, the foliar application of iron (Fe) in different forms and concentrations generated significant variations in chlorophyll and carotenoid content (Table 2). The IC100 treatment showed the highest values of chlorophyll b (2.9 μg cm^{-2} FW) and total chlorophyll (9.34 μg cm^{-2} FW), exceeding the control by approximately 10% and 9%, respectively. As for chlorophyll a, the highest content was recorded with IONPs25 (6.51 μg cm^{-2} FW), with an increase of nearly 9% compared to the control. Carotenoids also reached their highest value with IONPs25 (1.26 μg cm^{-2} FW, 17% more than the control). In contrast, IONPs100 significantly reduced all pigments evaluated, especially carotenoids (0.70 μg cm^{-2} FW, 35% less than the control).

Iron is essential for chlorophyll biosynthesis and the assembly of photosynthetic complexes, as it participates as a cofactor in the key enzymes of tetrapyrrole metabolism and in chloroplast function [37]. The improvement observed in the IC100 and IONPs25 treatments can be explained by the greater availability and assimilation of Fe, which favored

pigment synthesis and stability, optimizing light capture and photosynthetic efficiency [38]. In contrast, high concentrations of IONPs (IONPs100) could have induced toxicity or redox imbalance, interfering with pigment metabolism, and limiting their accumulation, as reported in studies on micronutrient excess in photosynthetic tissues [31].

Table 2. Effect of foliar application of different iron sources and concentrations on photosynthetic pigments (chlorophyll a, chlorophyll b, total chlorophyll, and carotenoids) in plant leaves (μg cm^{-2} FW). Values represent mean ± standard error. Different letters indicate statistically significant differences according to Tukey's test ($p \leq 0.05$).

Treatment	Chlorophyll [a] μg cm^{-2} FW	Chlorophyll [b] μg cm^{-2} FW	Total Chlorophyll μg cm^{-2} FW	Carotenoids μg cm^{-2} FW
Control	5.9938 ± 0.2335 [ab]	2.5471 ± 0.1209 [ab]	8.5409 ± 0.3545 [ab]	1.0770± 0.0601 [ab]
IC25	5.2984 ± 0.2234 [abc]	2.1760 ± 0.1242 [abc]	7.4744 ± 0.3478 [abc]	1.0249 ± 0.1242 [abc]
IC50	5.3067 ± 0.2150 [abc]	2.2238 ± 0.0782 [abc]	7.5306 ± 0.2932 [abc]	0.9292 ± 0.0221 [abc]
IC100	6.4367 ± 1.0687 [a]	2.9008 ± 0.8081 [a]	9.3376 ± 1.8768 [a]	1.0467 ± 0.8099 [a]
FS25	5.6351 ± 0.5159 [abc]	2.3539 ± 0.2671 [abc]	7.9890 ± 0.7830 [abc]	1.1358 ± 0.1157 [abc]
FS50	5.3402 ± 1.1897 [abc]	2.2876 ± 0.4731 [abc]	7.6278 ± 1.6628 [abc]	1.0773 ± 0.0001 [abc]
FS100	5.2843 ± 0.0244 [abc]	2.2399 ± 0.1747 [abc]	7.5242 ± 0.1991 [abc]	0.9184 ± 0.0226 [abc]
IONPs25	6.5089 ± 0.4016 [a]	2.8944 ± 0.2528 [a]	9.4034 ± 0.6545 [a]	1.2623 ± 0.2170 [a]
IONPs50	5.1449 ± 0.3743 [bc]	2.0594 ± 0.2083 [bc]	7.2044 ± 0.5826 [bc]	1.0139 ± 0.0052 [bc]
IONPs100	3.7069 ± 0.0001 [c]	1.4671 ± 0.1000 [c]	5.1740 ± 0.0023 [c]	0.7027 ± 0.0001 [c]

3.4. SPAD Values

Iron plays an essential role in chlorophyll synthesis, which is reflected in SPAD values and the photosynthetic capacity of plants, as it is a key component for the functioning of photosynthetic complexes and nitrogen metabolism [39]. In the present study, the foliar application of iron (Fe) in different forms and concentrations significantly increased SPAD values compared to the control (Figure 6). The control had an approximate value of 40 SPAD units (100%). The greatest increase was observed with IONPs25, which reached a value close to 54 SPAD units, representing a 36% increase over the control. The IC25, IC50, IC100, FS25, FS50, FS100, and IONPs100 treatments showed similar increases, ranging from 25% to 32%. IONPs25 showed an increase of 36%, placing it in the upper range of response.

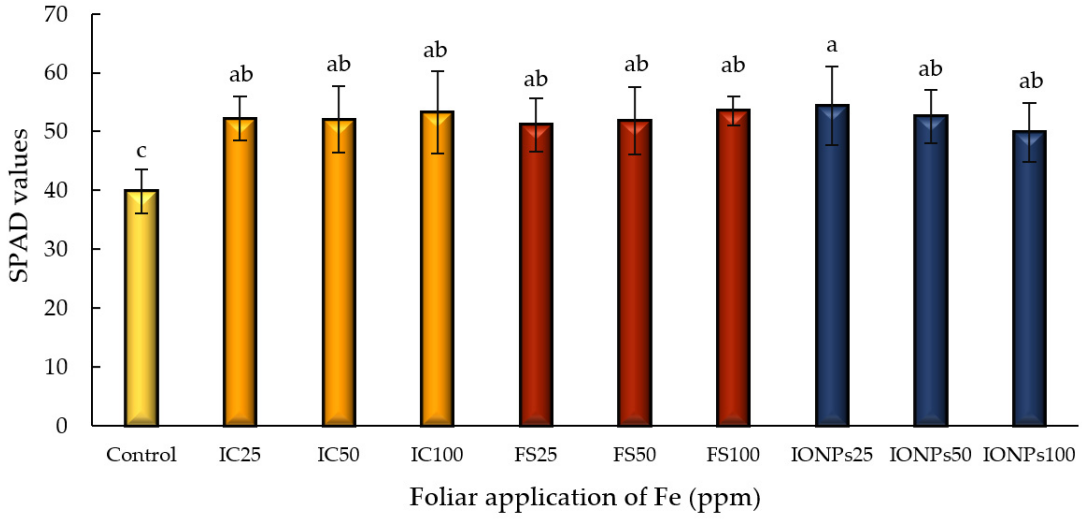

Figure 6. Effect of foliar application of iron chelate (Fe-EDDHA), ferric sulfate ($Fe_2(SO_4)_3$), and iron oxide nanoparticles (Fe_2O_3) on SPAD values of *Spinacia oleracea* L. cv. Viroflay plants. Different letters represent significant differences between treatments according to Fisher's LSD test ($p \leq 0.05$).

From a physiological point of view, these increases in SPAD values reflect a higher concentration of leaf chlorophyll, which is consistent with the essential role of Fe in chlorophyll synthesis and the formation of photosynthetic complexes. Iron acts as a cofactor for several enzymes involved in chloroplast assembly and electron transport during photosynthesis. In addition, an adequate Fe supply has been shown to improve photosynthetic efficiency and crop yield under stress conditions, such as salinity, by optimizing chlorophyll levels and leaf fluorescence properties [39]. Treatments with Fe nanoparticles, particularly IONPs25, may have favored greater Fe availability in leaf tissues, promoting the formation and stability of photosynthetic pigments [31]. These findings are consistent with studies on rice and other crops where the foliar application of Fe increased SPAD values and the photosynthetic rate [40].

3.5. Nitrate Reductase Activity

Iron plays a fundamental role in nitrate reduction, as it is an essential component of the prosthetic group of the enzyme nitrate reductase, which catalyzes the assimilation of inorganic nitrogen in plants [41]. This enzyme depends on heme cofactors and iron-sulfur centers, whose functionality is directly related to the availability of iron in plant tissue [42]. The activity of putative (real) nitrate reductase (NR_{act}) represents the active fraction of the enzyme under physiological conditions without the addition of external cofactors [43]. In the present study, significant differences among treatments were observed. The ferric sulfate treatment at 100 ppm (FS100) showed the highest activity, followed by iron nanoparticles at 25 ppm (IONPs25) and the control (Figure 7).

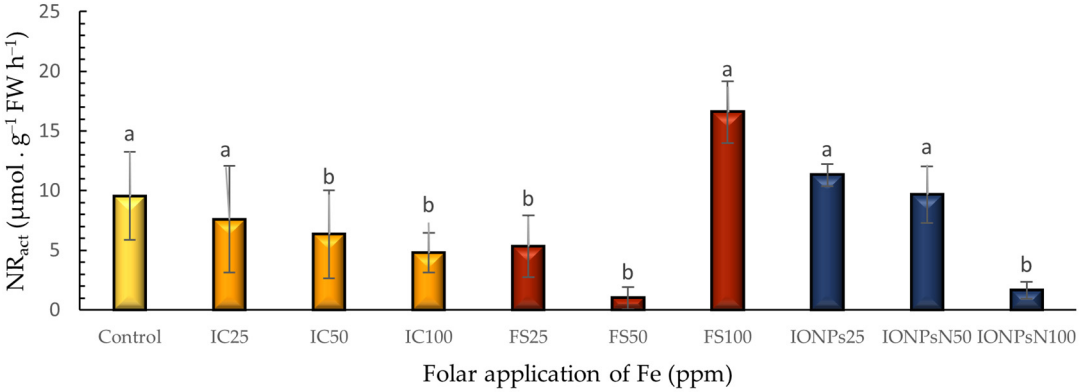

Figure 7. Effect of foliar application of iron chelate (Fe-EDDHA), ferric sulfate ($Fe_2(SO_4)_3$), and iron oxide nanoparticles (Fe_2O_3) on activity of putative (real) nitrate reductase (NR_{act}) of *Spinacia oleracea* L. cv. Viroflay plants. Different letters represent significant differences between treatments according to Fisher's LSD test ($p \leq 0.05$).

This indicates that, under these conditions, iron was sufficiently bioavailable to keep the enzyme active, promoting nitrate assimilation [2]. Conversely, treatments with iron chelate (Fe-EDDHA) at all concentrations tested (IC25, IC50, and IC100), as well as iron nanoparticles at 100 ppm (IONPs100) and ferric sulfate at 50 ppm (FS50), exhibited significantly lower levels of real activity, which could be associated with toxic effects due to excess iron. These results suggest that both the chemical form and dosage of iron influence the functional regulation of NR, and that high concentrations, particularly in nanoparticle form, may negatively affect the physiological activation of the enzyme [44].

Regarding the maximum nitrate reductase activity (NR_{max}), it represents the total amount of functional enzymes present in the tissue; that is, the maximum "potential" of NR [45]. In the present study notable variations were observed depending on the iron source and concentration applied (Figure 8). The IONPs50 treatment was the most

outstanding, with an increase of 246% compared to the control. FS25, FS50, FS100, and IC25 increased the activity by 110%, 77%, 115%, and 87%, respectively. In contrast, IC100 reduced the activity by 1% and 62%, respectively, compared to the control. IONPs25 and IONPs100 showed moderate increases of 72% and 70%, respectively. This increase in NR_{max} activity under IONPs application may be due to the improved nitrogen metabolism and increased Fe availability as an essential cofactor of the enzyme, thereby promoting nitrate assimilation [46]. It has been demonstrated that the application of IONPs enhances photosynthesis and nitrogen-use efficiency, both of which are directly correlated with increased NR activity [28]. According to Marschner [2], when plants properly assimilate nitrogen, this is directly reflected in higher yields. Therefore, the increase in activity observed in this treatment could be directly contributing to greater physiological efficiency and, consequently, higher yields. In contrast, the reductions observed with IC100 could be associated with a phytotoxic effect that inhibits NR activity [30].

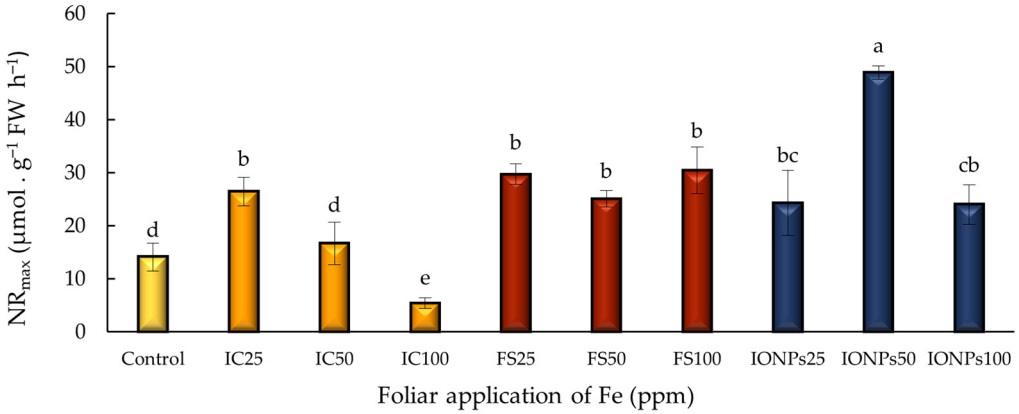

Figure 8. Effect of foliar application of iron chelate (Fe-EDDHA), ferric sulfate ($Fe_2(SO_4)_3$), and iron oxide nanoparticles (Fe_2O_3) on maximum nitrate reductase activity (NR_{max}) of *Spinacia oleracea* L. cv. Viroflay plants. Different letters represent significant differences between treatments according to Fisher's LSD test ($p \leq 0.05$).

Regarding the activation state of NR activity, defined as the ratio between putative (real) NR activity and maximum NR activity, this parameter is used to estimate the proportion of the NR enzyme that is active in the sample compared to its total potential (NR_{max}); in other words, it indicates the active fraction of NR [45]. In the present study, the treatment with iron chelate at 100 ppm (IC100) showed the highest activation state (89%) (Figure 9), suggesting efficient NR activation possibly associated with good iron availability and intracellular mobilization. In contrast, treatments with iron nanoparticles at 100 ppm (IONPs100) and ferric sulfate at 50 ppm (FS50) showed significantly lower values (less than 20%), indicating a low proportion of active enzymes. This behavior could be due to cellular stress caused by excess iron or a low effective availability at the enzymatic site. Both the form and concentration of iron influenced not only the total expression of the enzyme (maximum activity) but also its functional activation, highlighting the importance of considering post-translational regulation when evaluating the effectiveness of foliar micronutrient fertilization treatments [47]. Although the IONPs treatment at 100 ppm resulted in the greatest increase in total biomass (49.8%) and leaf yield (40%) compared to the control, a significant decrease in photosynthetic pigment content and nitrate reductase enzyme activity was also observed. The physiological effects observed following the application of iron oxide nanoparticles (IONPs) suggest a distinct behavior compared to conventional iron sources. At moderate concentrations (50 ppm), IONPs may act as a slow-release source of Fe^{3+}, enhancing nitrogen assimilation by maintaining optimal levels of bioavailable iron without inducing toxicity. Their nanoscale size facilitates foliar

penetration through cuticular pores or stomata, and subsequent translocation is likely mediated by apoplastic movement, as reported in several studies [12,31]. However, at higher concentrations (100 ppm), the excessive internalization of nanoparticles may disrupt redox homeostasis or cause oxidative stress, potentially inhibiting enzymatic processes such as nitrate reduction and degrading photosynthetic pigments. In contrast, Fe-EDDHA and $Fe_2(SO_4)_3$, being fully soluble, follow classical ionic absorption routes through the apoplast, which may explain their distinct physiological responses at similar concentrations [12]. These differences highlight the need for a better understanding of the nanoparticle–plant interface and the fine balance between beneficial and toxic thresholds in nano-enabled foliar fertilization. Therefore, future research should aim to precisely define the concentration threshold at which foliar iron nanoparticles shift from beneficial to detrimental effects.

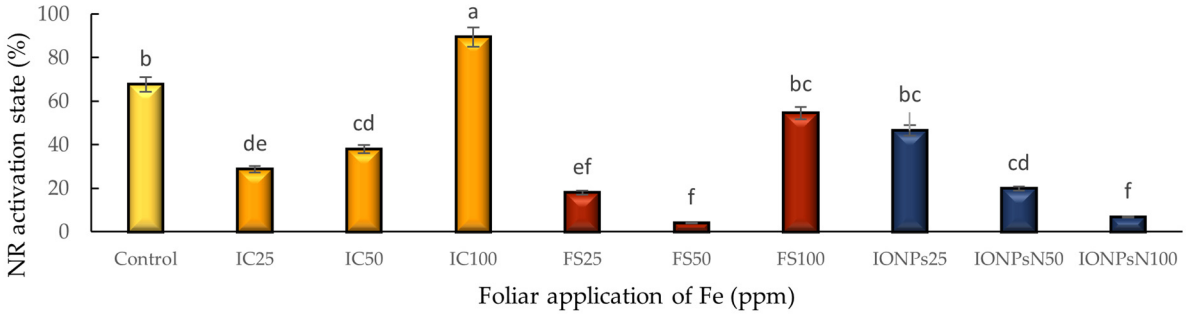

Figure 9. Effect of foliar application of iron chelate (Fe-EDDHA), ferric sulfate ($Fe(SO_4)_3$), and iron oxide nanoparticles (Fe_2O_3) on the activation state of NR in plants of *Spinacia oleracea* L. cv. Viroflay. Different letters represent significant differences between treatments according to Fisher's LSD test ($p \leq 0.05$).

3.6. Soluble Amino Acids

Iron is involved in various metabolic processes, precursors of soluble amino acid synthesis, essential for plant growth and development [48]. In the present study, the concentration of soluble amino acids varied significantly in response to the foliar application of Fe (Figure 10). The control had a value of approximately 0.76 mg g^{-1} FW (100%). The greatest increase was observed with FS50, which reached about 1.3 mg g^{-1} FW, representing a 68% increase over the control. IC100 produced a 63% increase, while IC50 and IONPs100 increased by 29% and 26%, respectively. IONPs25 showed a 34% increase, while IC25 and FS25 showed values similar to the control. In contrast, FS100 and IONPs50 showed no improvement, remaining at the same level as the control.

The increase in soluble amino acids observed with FS50 and IC100 could be explained by the role of Fe in the activation of key enzymes in nitrogen metabolism, favoring the synthesis of nitrogenous compounds such as amino acids [28]. Similarly, Fe application has been associated with the increased photosynthetic activity and primary metabolism, which translates into greater amino acid accumulation in young tissues [12]. However, high concentrations of conventional Fe or the application of certain forms of nanoparticles could lead to nutritional imbalances or oxidative stress, which would limit the accumulation of these compounds. These variations may be related to a physiological response to oxidative stress, as plants can increase the synthesis of specific proteins as an adaptive mechanism, including antioxidant enzymes and defense proteins that influence the metabolic resilience of crops [49].

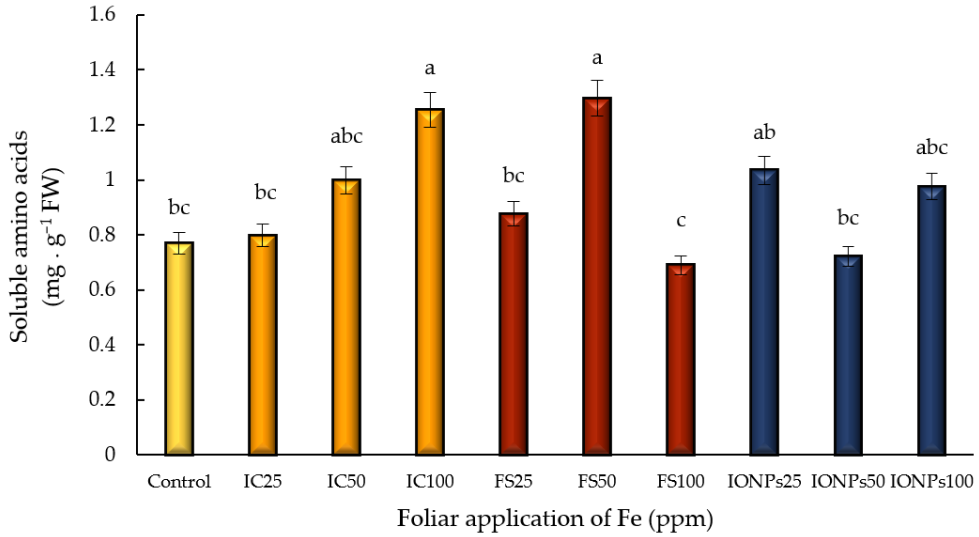

Figure 10. Effect of foliar application of iron chelate (Fe-EDDHA), ferric sulfate ($Fe_2(SO_4)_3$), and iron oxide nanoparticles (Fe_2O_3) on the concentration of soluble amino acids in plants of *Spinacia oleracea* L. cv. Viroflay. Different letters represent significant differences between treatments according to Fisher's LSD test ($p \leq 0.05$).

3.7. Soluble Proteins

Iron is involved in various metabolic processes, including those that regulate homeostasis and the synthesis of soluble proteins, which are essential for plant growth and development, as it acts as a cofactor and regulator at the protein level [50].

In the present study, the concentration of soluble protein showed significant variations depending on the type and concentration of Fe applied. The control showed a value of approximately 23.7 mg g^{-1} FW (100%) (Figure 11). The greatest increase was observed with FS50, reaching about 37.8 mg g^{-1} FW, representing a 59% increase over the control. This was followed by IC100 and FS25, with increases of 53% and 344%, respectively. IC25, IC50, FS100, IONPs25, and IONPs100 showed moderate increases of 19% to 25%. In contrast, IONPs50 decreased by 10.1% compared to the control.

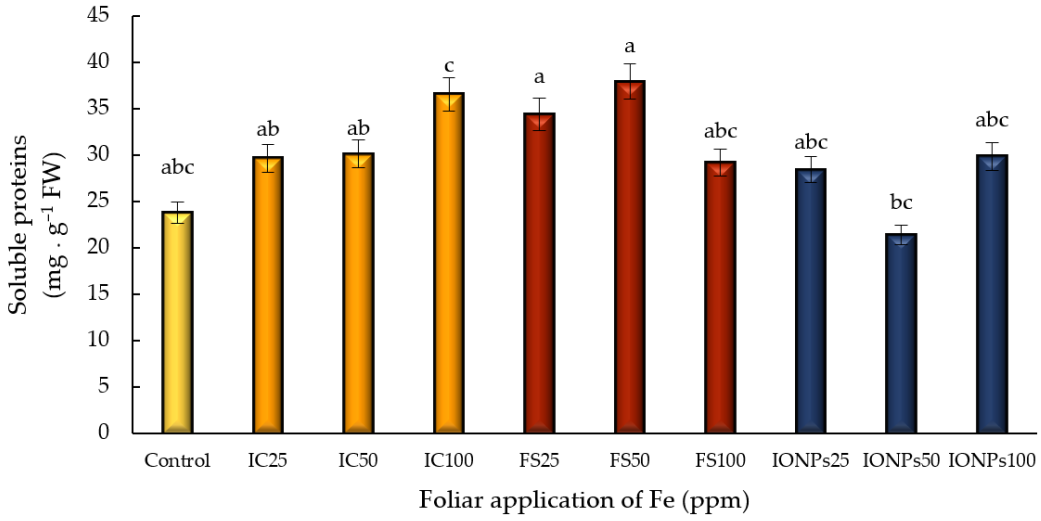

Figure 11. Effect of foliar application of iron chelate (Fe-EDDHA), ferric sulfate ($Fe_2(SO_4)_3$), and iron oxide nanoparticles (Fe_2O_3) on the concentration of soluble proteins in plants of *Spinacia oleracea* L. cv. Viroflay. Different letters represent significant differences between treatments according to Fisher's LSD test ($p \leq 0.05$).

The increase in soluble protein under certain treatments could be explained by the role of Fe in activating metabolic pathways that stimulate protein synthesis, particularly under conditions that favor growth and development [42]. The availability of Fe as a cofactor in key enzymes and its role in nitrogen metabolism contribute to the accumulation of soluble proteins in tissues [37].

4. Conclusions

The foliar application of iron oxide nanoparticles (IONPs) in *Spinacia oleracea* L. promoted greater nitrogen assimilation efficiency, evidenced by significant increases in nitrate reductase activity (NR activity up to 246% with 50 ppm IONPs), biomass accumulation (up to 50% with 100 ppm IONPs), and soluble protein content, along with improvements in photosynthetic pigments and SPAD values. Doses of 50–100 ppm of IONPs produced superior physiological responses compared to conventional iron sources, such as iron chelate (Fe-EDDHA) and ferric sulfate ($Fe_2(SO_4)_3$), without causing evident phytotoxic effects. However, the results also indicate that the effectiveness of each iron source depends not only on its chemical form but also on the applied concentration. High doses of chelate (IC100) and IONPs (IONPs100) showed physiological limitations, which may be associated with oxidative stress or iron toxicity. This underscores the importance of establishing optimal application ranges and considering both the physiological response and crop type. Altogether, these findings reinforce the potential of IONPs as an innovative and sustainable alternative to enhance nitrogen nutrition and yield in leafy vegetables. Nevertheless, further long-term studies under field conditions are required to validate these effects and develop safe and efficient application protocols for agricultural practice.

Author Contributions: The authors confirm their contribution to the paper as follows: study conception and design: C.L.F.-L. and E.S.; data collection: C.L.F.-L. and E.H.O.-C.; analysis and interpretation of results: C.L.F.-L., E.N.-L., A.G.-A., C.C.-M., E.M.-M., M.I.T.-G. and E.H.O.-C.; draft manuscript preparation: C.L.F.-L., M.I.T.-G., E.N.-L., and E.S. All authors have read and agreed to the published version of the manuscript.

Funding: This research received no external funding.

Data Availability Statement: The authors declare that all data discussed in this study are available in the manuscript.

Acknowledgments: We would like to thank the Secretaría de Ciencia, Humanidades, Tecnología e Innovación (SECIHTI—Mexico) for the support provided by the scholarship granted to Cristina Larissa Franco Lagos through the "Becas Nacionales SECIHTI" program with CVU No. 1321537.

Conflicts of Interest: The authors declare no conflicts of interest.

References

1. Liu, X.; Zhang, Y.; Han, W.; Tang, A.; Shen, J.; Cui, Z.; Zhang, F. Enhanced nitrogen deposition over China. *Nature* **2010**, *494*, 459–462. [CrossRef]
2. Marschner, P. *Marschner's Mineral Nutrition of Higher Plants*, 3rd ed.; Academic Press: London, UK, 2012.
3. Broadley, M.R.; Brown, P.R.; Cakmak, I.; Rengel, Z.; Zhao, F.J. Function of nutrients: Micronutrients. In *Marschner's Mineral Nutrition of Higher Plants*, 3rd ed.; Marschner, P., Ed.; Academic Press: London, UK, 2012; pp. 191–248.
4. Briat, J.F.; Curie, C.; Gaymard, F. Iron utilization and metabolism in plants. *Curr. Opin. Plant Biol.* **2007**, *10*, 276–282. [CrossRef]
5. Guerinot, M.L.; Yi, Y. Iron: Nutritious, noxious, and not readily available. *Plant Physiol.* **1994**, *104*, 815–820. [CrossRef] [PubMed]
6. Tawfik, M.M.; Mohamed, M.H.; Sadak, M.S.; Thalooth, A.T. Iron oxide nanoparticles effect on growth, physiological traits, and nutritional contents of *Moringa oleifera* grown in saline environment. *Bull. Natl. Res. Cent.* **2021**, *45*, 177. [CrossRef]
7. Mondal, A.; Paul, S.; Pal, R.; Paul, S. Nano iron loaded algal biomass: For better yield, amino acid, and iron content in rice—A 'nano-phycofertilizer'. *Algal Res.* **2024**, *81*, 103573. [CrossRef]

8. Ahmed, M.A.; Shafiei-Masouleh, S.-S.; Mohsin, R.M.; Salih, Z.K. Foliar application of iron oxide nanoparticles promotes growth, mineral contents, and medicinal qualities of *Solidago virgaurea* L. *J. Soil Sci. Plant Nutr.* **2023**, *23*, 2610–2624.
9. Guillén-Enríquez, R.R.; Zuñiga-Estrada, L.; Ojeda-Barrios, D.L.; Rivas-García, T.; Trejo-Valencia, R.; Preciado-Rangel, P. Effect of nano-biofortification with iron on yield and bioactive compounds in cucumber. *Rev. Mex. Cienc. Agríc.* **2022**, *13*, 173–184.
10. Gutiérrez-Ruelas, N.J.; Palacio-Márquez, A.; Sánchez, E.; Muñoz-Márquez, E.; Chávez-Mendoza, C.; Ojeda-Barrios, D.L.; Flores-Córdova, M.A. Impact of the foliar application of nanoparticles, sulfate and iron chelate on the growth, yield and nitrogen assimilation in green beans. *Not. Bot. Horti Agrobot. Cluj-Napoca* **2021**, *49*, 12437. [CrossRef]
11. Lindsay, W.L.; Schwab, A.P. The chemistry of iron in soils and its availability to plants. *J. Plant Nutr.* **1982**, *5*, 821–840. [CrossRef]
12. Feng, Y.; Kreslavski, V.D.; Shmarev, A.N.; Ivanov, A.A.; Zharmukhamedov, S.K.; Koso-bryukhov, A.; Yu, M.; Allakhverdiev, S.I.; Shabala, S. Effects of Iron Oxide Na-noparticles (Fe_3O_4) on Growth, Photosynthesis, Antioxidant Activity and Distribution of Mineral Elements in Wheat (*Triticum aestivum*) Plants. *Plants* **2022**, *11*, 1894. [CrossRef]
13. Rico, C.M.; Majumdar, S.; Duarte-Gardea, M.; Peralta-Videa, J.R.; Gardea-Torresdey, J.L. Interaction of nanoparticles with edible plants and their possible implications in the food chain. *J. Agric. Food Chem.* **2011**, *59*, 3485–3498. [CrossRef]
14. Li, L.; Huang, Z.; Zhou, Z.; Tao, Y.; Zhang, Y.; Mu, Y.; Wu, S.; Nie, L. Foliar Application of Zinc Oxide Nanoparticles Improved Yield and 2-Acetyl-1-pyrroline Content in Fragrant Rice under Salt Stress. *Crop Environ.* **2025**, *4*, 107–117. [CrossRef]
15. Murcia, M.A.; Jiménez-Monreal, A.M.; González, J.; Martínez-Tomé, M. Spinach (*Spinacia oleracea* L.). In *Nutritional Composition and Antioxidant Properties of Fruits and Vegetables*; Jaiswal, A.K., Ed.; Academic Press: London, UK, 2020; pp. 181–195.
16. Santamaria, P.; Campanile, G.; Parente, A.; Elia, A. Subirrigation vs drip-irrigation: Effects on yield and quality of soilless grown cherry tomato. *J. Hortic. Sci. Biotechnol.* **2003**, *78*, 290–296. [CrossRef]
17. Sánchez, E.; Ruiz, J.M.; Romero, L. Proline metabolism in response to nitrogen toxicity in fruit of French Bean plants (*Phaseolus vulgaris* L. cv Strike). *Sci. Hortic.* **2002**, *93*, 225–233. [CrossRef]
18. Waqas Mazhar, M.; Ishtiaq, M.; Hussain, I.; Parveen, A.; Hayat Bhatti, K.; Azeem, M.; Thind, S.; Ajaib, M.; Maqbool, M.; Sardar, T. Seed nano-priming with zinc oxide nanoparticles in rice mitigates drought and enhances agronomic profile. *PLoS ONE* **2022**, *17*, e0264967. [CrossRef]
19. Schucknecht, A.; Hammerle, A.; Wohlfahrt, G.; Tappeiner, U.; Wieser, G. Estimating dry biomass and plant nitrogen concentration in pre-Alpine grassland vegetation. *Biogeosciences* **2022**, *19*, 2699–2717. [CrossRef]
20. Wellburn, A.R. The spectral determination of chlorophylls a and b, as well as total carotenoids, using various solvents with spectrophotometers of different resolution. *J. Plant Physiol.* **1994**, *144*, 307–313. [CrossRef]
21. Shrestha, S.; Brueck, H.; Asch, F. Chlorophyll index, photochemical reflectance index and chlorophyll fluorescence measurements of rice leaves supplied with different N levels. *J. Photochem. Photobiol. B Biol.* **2012**, *113*, 7–13. [CrossRef]
22. Kaiser, W.M.; Brendle-Behnisch, E. Acid-base-modulation of nitrate reductase in leaf tissues. *Planta* **1995**, *196*, 1–6. [CrossRef]
23. Yemm, E.W.; Cocking, E.C.; Ricketts, R.E. The determination of amino-acids with ninhydrin. *Analyst* **1955**, *80*, 209–214. [CrossRef]
24. Bradford, M.M. A rapid and sensitive method for the quantitation of microgram quantities of protein utilizing the principle of protein-dye binding. *Anal. Biochem.* **1976**, *72*, 248–254. [CrossRef]
25. SAS Institute Inc. *SAS/STAT® 15.2 User's Guide*; SAS Institute Inc.: Cary, NC, USA, 2021.
26. Singh, S.P.; Dutta, S.K.; Jha, S.; Prasad, S.S. Nutrient management in calcareous soil improves rice–maize sustainable yield index, performance indicators. *Commun. Soil Sci. Plant Anal.* **2021**, *52*, 701–716. [CrossRef]
27. Dos Santos, V.R.; Costa, L.C.; Rocha, A.M.S. Biomass accumulation, extraction and nutrient use efficiency by cover crops. *Res. Soc. Dev.* **2020**, *9*, e9433108811. [CrossRef]
28. Yousaf, N.; Ishfaq, M.; Qureshi, H.A.; Saleem, A.; Yang, H. Characterization of root and foliar-applied iron oxide nanoparticles (α-Fe_2O_3, γ-Fe_2O_3, Fe_3O_4, and bulk Fe_3O_4) in improving maize (*Zea mays* L.) growth and physiology. *Nanomaterials* **2023**, *13*, 3036. [CrossRef] [PubMed]
29. Cao, X.; Yue, L.; Wang, C.; Luo, X.; Zhang, C.; Zhao, X.; Wu, F. Foliar application with iron oxide nanomaterials stimulate nitrogen fixation, yield, and nutritional quality of soybean. *ACS Nano* **2022**, *16*, 8500–8514. [CrossRef] [PubMed]
30. Mahmoud, A.W.M.; Ayad, A.A.; Abdel-Aziz, H.S.M. Foliar application of different iron sources improves morpho-physiological traits and nutritional quality of broad bean grown in sandy soil. *Plants* **2022**, *11*, 2599. [CrossRef] [PubMed]
31. Tombuloglu, G.; Tombuloglu, H.; Slimani, Y. Effects of foliar iron oxide nanoparticles (Fe_3O_4) application on photosynthetic parameters, distribution of mineral elements, magnetic behaviour, and photosynthetic efficiency. *Eur. J. Agron.* **2024**, *149*, 126849.
32. Nasar, J.; Wang, G.-Y.; Zhou, F.-J.; Gitari, H.; Zhou, X.-B.; Tabl, K.M.; Hasan, M.E.; Ali, H.; Waqas, M.M.; Ali, I.; et al. Nitrogen fertilization coupled with iron foliar application improves the photosynthetic characteristics, photosynthetic nitrogen use efficiency, and the related enzymes of maize crops under different planting patterns. *Front. Plant Sci.* **2022**, *13*, 988055. [CrossRef]
33. Drostkar, E.; Talebi, R.; Kanouni, H. Foliar application of Fe, Zn and NPK nano-fertilizers on seed yield and morphological traits in chickpea under rainfed condition. *J. Resour. Ecol.* **2016**, *4*, 221–228.
34. Dola, D.B.; Mannan, M.A.; Sarker, U.; Mamun, M.A.A.; Islam, T.; Ercisli, S.; Marc, R.A. Nano-iron oxide accelerates growth, yield, and quality of *Glycine max* seed in water deficits. *Front. Plant Sci.* **2022**, *13*, 992535. [CrossRef]

35. Rui, M.; Ma, C.; Hao, Y.; Guo, J.; Rui, Y.; Tang, X.; Zhu, S. Iron oxide nanoparticles as a potential iron fertilizer for peanut (*Arachis hypogaea*). *Front. Plant Sci.* **2016**, *7*, 815. [CrossRef]
36. Gao, D.; Ran, C.; Zhang, Y.; Wang, X.; Lu, S.; Geng, Y. Effect of different concentrations of foliar iron fertilizer on chlorophyll fluorescence characteristics of iron-deficient rice seedlings under saline sodic conditions. *Eur. J. Agron.* **2022**, *135*, 126492. [CrossRef] [PubMed]
37. Kroh, G.E.; Pilon, M. Regulation of iron homeostasis and use in chloroplasts. *Int. J. Mol. Sci.* **2020**, *21*, 3395. [CrossRef] [PubMed]
38. Higuchi, K.; Saito, A. Elucidation of efficient photosynthesis in plants with limited iron. *Soil Sci. Plant Nutr.* **2022**, *68*, 556–567. [CrossRef]
39. Chen, J.; Zhang, N.N.; Pan, Q.; Lin, X.Y.; Shangguan, Z. Hydrogen sulphide alleviates iron deficiency by promoting iron availability and plant hormone levels in *Glycine max* seedlings. *BMC Plant Biol.* **2020**, *20*, 467. [CrossRef]
40. Aouada, F.A.; de Moura, M.R. Nanotechnology Applied in Agriculture: Controlled Release of Agrochemicals. In *Nanotechnologies in Food and Agriculture*; Rai, M., Ribeiro, C., Mattoso, L., Duran, N., Eds.; Springer: Cham, Switzerland, 2015; pp. 103–118.
41. Yaneva, I.A.; Baydanova, V.D.; Vunkova Radeva, R.V. Nitrate reductase activation state in leaves of molybdenum deficient winter wheat. *J. Plant Physiol.* **2000**, *157*, 495–501. [CrossRef]
42. Campbell, W.H. Nitrate reductase structure, function and regulation: Bridging the gap between biochemistry and physiology. *Annu. Rev. Plant Physiol. Plant Mol. Biol.* **1999**, *50*, 277–303.
43. Tejada-Jimenez, M.; Llamas, A.; Galván, A.; Fernández, E. Role of Nitrate Reductase in NO Production in Photosynthetic Eukaryotes. *Plants* **2019**, *8*, 56. [CrossRef]
44. Gohar, F.; Iqbal, U.; Khan, M.B.; Rehman, F.; Maryam, F.; Azmat, M.; Munir, S.; Shahid, M. Impact of Nanoparticles on Plant Growth, Development and Physiolo-gical Processes: A Comprehensive Review. *SM J. Med. Plant Stud.* 2025, *in press*.
45. Correia, M.J.; Fonseca, F.; Azedo-Silva, J.; Dias, C.; David, M.M.; Barrote, I.; Osório, M.L.; Osório, J. Effects of water deficits on the activity of nitrate reductase and content of sugars, nitrate and free amino acids in the leaves and roots of sunflower and white lupin plants growing under two nutrient supply regimes. *Physiol. Plant.* **2005**, *123*, 190–203. [CrossRef]
46. Borlotti, A.; Vigani, G.; Zocchi, G. Iron deficiency affects nitrogen metabolism in cucumber (*Cucumis sativus* L.) plants. *BMC Plant Biol.* **2012**, *12*, 189. [CrossRef]
47. Kaiser, W.M.; Huber, S.C. Post-translational regulation of nitrate reductase: Mechanism, physiological relevance and environmental triggers. *J. Exp. Bot.* **2001**, *52*, 1981–1989. [CrossRef]
48. Ning, X.; Lin, M.; Huang, G.; Mao, J.; Gao, Z.; Wang, X. Research progress on iron absorption, transport, and molecular regulation strategy in plants. *Front. Plant Sci.* **2023**, *14*, 1190768. [CrossRef]
49. Rao, M.J.; Duan, M.; Zhou, C.; Jiao, J.; Cheng, P.; Yang, L. Antioxidant defense system in plants: Reactive oxygen species production, signaling, and scavenging during abiotic stress-induced oxidative damage. *Horticulturae* **2025**, *11*, 477. [CrossRef]
50. Zhang, X.; Xue, C.; Wang, R.; Shen, R.; Lan, P. Physiological and proteomic dissection of the rice roots in response to iron deficiency and excess. *J. Proteom.* **2022**, *258*, 104567. [CrossRef]